PROCEEDINGS OF ECOS 2023 - THE 36TH INTERNATIONAL CONFERENCE ON
EFFICIENCY, COST, OPTIMIZATION, SIMULATION AND ENVIRONMENTAL IMPACT OF ENERGY SYSTEMS
25-30 JUNE, 2023, LAS PALMAS DE GRAN CANARIA, SPAIN

Performance comparison of cold thermal storage for gas turbine inlet cooling with traditional energy storage technologies in current electricity markets

Alberto Vannoni[a], and Alessandro Sorce[b]

[a] University of Genova, Genova, Italy, alberto.vannon@edu.unige.it, CA,
[b] University of Genova, Genova, Italy, alessandro.sorce@unige.it

Abstract:

In the current electricity grids, it is becoming pivotal to install a large amount of storage capacity in order to maximize the deployment of renewable energy sources, stabilize the grid, and mitigate electricity price volatility. Engineering research focused on improving storage technologies performance aiming to improve the round trip efficiency and increase the utilization opportunities. Besides storage implementation, power plant flexibility is pursued as well to support electricity grids in the transient stage towards a decarbonized energy mix. Recent studies have investigated the possibility of enhancing the flexibility of Combined Cycle Gas Turbine (CCGT) power plants by means of a heat pump and a cold thermal energy storage, this solution demonstrated a relevant potential, especially in those locations characterized by warm climates and volatile electricity markets. In such a situation is possible to fully exploit the cold thermal energy storage, decreasing the net power output, during storage charging in off-peak periods, and boosting it, through inlet cooling, during the most profitable periods. This paper performs a techno-economic comparison between cold thermal energy storage for gas turbines air inlet cooling and other established energy storage technologies (such as pumped hydro, batteries, compressed air, and pumper thermal storage) for time load shifting and energy arbitrage on the day ahead market. The analysis is based on Linear Programming (LP) and Mixed Integer Linear Programming (MILP) models for the optimization of the dispatch. The impact of market parameters on storage technologies performance is investigated and discussed, selecting the best option for each considered scenario.

Keywords:

Storage; Flexibility; CCGT; Heat Pump; Optimization; Electricity Market;

1. Introduction

The awareness about the ongoing climate change due to emissions of Green House Gasses (GHG) has led in the last decades almost every country to pledge drastic GHG emission cuts [1] and a complete transition to a decarbonized economy is commonly scheduled for the horizon of 2050 or 2070 [2]. The first step of the Energy Transition has been the massive installation of electricity generation capacity from Renewable Energy Sources (RES). Approximately 2 TW have been installed globally in the period 2010-20, and the overall share of electricity generation from RES reached 28%, overcoming 40% in many advanced economies even considering a significant contribution of hydropower [3]. Even a higher amount of RES capacity is forecast to be installed in the near future (between 2.4 and 3.7 TW by 2027 [4]); indeed, carbon intensity targets have been set more and more challenging and the demand for low-carbon electricity is expected to grow following the coupling of different energy sectors, such as Heating or Transportation [5].

Nevertheless, since the hydropower growth potential is limited, most RES capacity addiction depends on solar and wind sources, strongly characterized by discontinuity and stochasticity. Although forecasting of RES production in advance has improved significantly, especially thanks to artificial intelligence and data-driven modeling [6,7], the mismatch between demand and production remains a severe issue and a significant amount of green electricity is often curtailed because of an overgeneration or a lack of transportation capacity of electricity grids [8]. Curtailments are negligible for PV generation but are relevant for wind, Especially in countries characterized by high wind energy shares, i.e., above 30%, up to 10% of wind generation can be curtailed [9]. Within this context, energy storage became a pivotal technology that must be implemented massively at the grid scale to support the energy transition and maximize the dispatch of renewable energy [10]. To be impactful on energy system management, storage must present adequate both power and energy sizes, there is no unique definition of grid-scale storage size. However, in this paper, 1 MW discharge power for at least 1h is assumed as a threshold value. For such applications pumped hydro,

https://doi.org/10.52202/069564-0213

electrochemical batteries, compressed air, and pumped thermal energy storages are the most promising technologies, there many other solutions have been investigated, but currently present a too-low technology readiness level (TRL) on such a scale.

Besides bulk energy arbitrage, i.e., the action of buying cheap energy during off-peak price periods, storing it, and selling it during price-peaking periods, storage technologies can be employed to provide services to the grid. This paper focuses only on load time shifting by energy arbitrage as the most relevant use considering the energy involved and the pivotal importance to maximize the RES dispatch and reduce the carbon footprint of electricity generation.

Historically the first form of energy storage implemented on a large scale was pumped hydroelectric storage (PHS), it represents a variation of conventional reservoir hydroelectric power plants. Energy is stored in the form of potential energy of water that is pumped from a lower reservoir to an upper reservoir [11]. PHS is a consolidated technology, already implemented widely at the grid scale since the 1970s to absorb the excess base load production from coal and nuclear power plants [12]. PHS plants have been installed especially in those regions characterized by an existing hydroelectric potential, such as the Alps in Europe, and along both the East and West Coast in the US [13]. However, within a liberalized electricity market, oligopolistic ownership, especially if both PHS and conventional power plants are managed by the same operator, may lead to an under-exploitation of it, as in the case of Italy [14]. In fact, a strategic operation of PHS could reflect in social welfare losses [15]. From a technological perspective, PHS is characterized by a Round Trip Efficiency (RTE) typically ranging between 70% and 80% even if up to 87% have been claimed [11]. One of the major issues of PHS implementation concerns site identification that must satisfy criteria of technical and economic feasibility together with social acceptance. A systematic approach for new PHS site identification has been developed and applied by Connolly et al. [16]. An interesting variance application concerns seawater PHS whose main advantage is to be not subject to the constraint of water availability in the lower reservoir [17].

Battery Energy Storage (BES) are probably the technology expected to grow more in the next years. The International Energy Agency states that, according to the Net *zero emission by 2050* scenario, 680 GW of BES must be installed by 2030. 16 GW were already installed in 2021 [18]. Various BES types exist, the most interesting for large-scale applications include lithium-ion (Li-ion), sodium-sulfur (NaS), lead acid (Pb-acid), lead-carbon batteries, as well as zebra batteries (Na-$NiCl_2$), and flow batteries. Li-ion BESs represent almost the totality of installed grid-scale capacity (92% in the US [19]) mainly because of the round trip efficiency of up to 97% DC-DC [20,21], corresponding to 85-95% AC-AC [22]. NaS batteries are available since the early 2000s at MW scale [23] and are particularly appreciated for their achievable depth of discharge (up to 90%) [21], while the main drawback is the thermal management since they operate in the range of 300-350°C, causing up to 20% per day of parasitic losses during idle periods [24]; similar issues are presented by Zebra BES [23]. Lead-acid BESs are appreciated for their high recyclability [25] and reduced CAPEX even if characterized by a reduced lifespan [21]. Flow batteries use aqueous electrolytes with one or more dissolved active species; the electrolytes are stored in tanks, and, pumped through an electrochemical cell where energy conversion takes place, because of this architecture this kind of battery shows a unique capability to decouple energy and power [26], however, they are characterized by significantly higher energy density and lower efficiency. Vanadium redox flow batteries show the best values of RTE but are still limited to 75-85% [27]. A relevant issue of BES is the relevance of system degradation and aging: this strongly depends on usage mode and should be considered for optimal dispatch [28].

Compressed air Energy Storage (CAES), store energy as compressed air, for large applications typically underground reservoir are used. Even if porosity and permeability are mandatory requirements, geological constraints are not as strict as for PHS [29]. The clean medium, the moderate CAPEX for a unit of stored energy, and scalability are the most appreciated features. In contrast, low RTE, reduced depth of discharge, and a considerable response time are the main drawbacks [30]. RTE may be increased by advanced techniques for managing heat generated during the compression phase. According to these, CAPEX can be classified into Diabatic-CAES, more mature but less efficient, wasting compression heat and burning fuel, typically natural gas to preheat air before the expansion during the discharge phase, Adiabatic-CAES adopting a TES to store the compression heat and release it during the expansion without any fuel consumption, and Isothermal-CAES claiming RTE up to 70% but characterized by low TRL [31].

Pumped Thermal Energy Storage (PTES), also known as Carnot Batteries, is a type of energy storage system that uses thermal energy to store and release energy. PTES systems store energy by pumping a heat transfer fluid between two reservoirs at different temperatures. During the charging phase, power is used to drive a heat pump and transfer heat from the colder reservoir to the hotter one. To discharge the storage, the process is reversed, and the heat transfer fluid is pumped back from the hotter reservoir to the colder one, generating electricity in the process. PTES potential advantages for grid-scale applications include long cycle life, low life-cycle environmental impact, and appreciable energy density. However, the main drawback is a low RTE, which is typically in the range of 40-70% [32]. Additionally, PTES implies relevant specific CAPEX €/kW for the power and charging unit. PTES can be classified according to the discharging method, exploiting Brayton or Rankine cycles; the charging methods, mainly including reverse

https://doi.org/10.52202/069564-0213

thermodynamic cycles and or the use of electrical resistance; and type of Thermal Energy Storage (TES), sensible, latent, or chemical [33,34].

Besides these technologies, an interesting application was studied in recent years to couple a Combined Cycle Gas Turbine (CCGT) with an Inlet Conditioning Unit (ICU) consisting of a heat pump (HP) and a cold (5°C) TES, connected as in the scheme (Figure 1). The ICU could work i) continuously, employing the HP to conditionate the CCGT intake, ii) as equivalent energy storage indeed using cheap electricity to drive the HP and charge the cold TES and using it to cool down the CCGT intake and boost the power output during the price peak periods without additional auxiliary losses. Preliminary works assessed the impact of intake temperature on the CCGT performance to investigate the potentialities of an ICU integration [35]. Subsequently, by means of a Mixed Integer Linear Programming (MILP) approach, it was developed a methodology to optimize the scheduling of an integrated ICU-CCGT power plant on the day-ahead market only [36] or considering the potentialities from an ancillary services provision [37]. Finally, a comprehensive assessment was carried out considering different European and US market and climate scenarios [38]. Considering that an ICU can be installed retrofitting existing CCGT plants and that those plants currently represent the backbone of many electrical systems, installing an ICU is equivalent to an investment in energy storage technology since it may be employed for the purpose of energy arbitrage and increasing the ability of the plant to supply grid services.

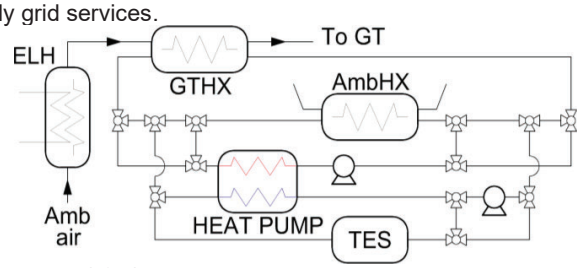

Figure. 1. Inlet Conditioning Unit (ICU) scheme

The present paper aims to carry out a marked-based economic comparison between grid-scale available storage technologies, including the ICU-CCGT integration. Even if the participation of storage in the flexibility markets is today an interesting perspective, such markets are strongly characterized by uncertainties and are hard to generalize among different country rules, therefore the proposed comparison only considers the possibility for storage to perform energy arbitrage on the day-ahead market. The novelty of the approach is to compare pure storage technologies against a flexible solution for refitting CCGT.

2. Methodology

A previous work identifies 9 market clusters in Europe and USA characterized by similar profit opportunities for ICU-CCGT integration [38]. In this paper, a techno-economic comparison between available grid-scale storages is carried out on the same markets (i.e., the centroids of previously identified clusters). The approach consists in determining the best scheduling of dispatch for each storage maximizing the Net Operational Profits (NetOP). Historical electricity price data have been used for this purpose [39,40]. Net Operational Profits are then used to compute techno-economic indicators: Pay Back Period (PBP) and Internal Rate of Return (IRR) are used for the economic assessment because of their independency of the storage size and the interest rate. Net Operational Profits, eq. (1), are defined as Revenues from selling electricity minus costs of charging and any cost associated with the degradation of the storage itself. Equations (2) define the PBP, and equation (3) the NPV such as the IRR is the value of i to which it follows NPV=0. Where N is the lifetime in years.

$$NetOP = \sum \left(Revenue - C_{charging} - C_{degr}\right) = \sum \left(OP - C_{degr}\right) \quad (1)$$

$$PBP = \frac{CAPEX}{OP_N} \quad (2)$$

$$NPV = -CAPEX + \sum_{n=1}^{N} \frac{OP_n}{(1+i)^n} \quad (3)$$

Storage operations are scheduled daily adopting an hourly resolution and an optimization horizon of 36h, as suggested by Vasylyev et al. [41]. According to this strategy price information beyond the daily horizon is provided to the optimizer. While the output concerning the first 24h is maintained, the scheduling from the 25th to the 36th will be overwritten by the following day optimization.

For the ICU-CCGT integration, the optimization of dispatch is carried out by means of the developed Mixed Integer Linear Programming (MILP) optimizer presented in detail by Mantilla et al. [36], and updated in the following works [37,38]. The objective function, equation (4) accounts for electricity price [39,40], gas cost (assumed as Henry Hub and TTF spot price for US and Europe respectively), CO_2 emission allowance cost [42], O&M cost, and cost associated with start-ups.

https://doi.org/10.52202/069564-0213

$$max \sum_{i=1}^{36} p_{el_i} \cdot (P_i^{out} - P_i^{HP} - Q_i^{elh}) - C_{gas_i} \cdot (Q_i^{fuel}) - C_{hs} V_{ji}^h - C_{ws} \cdot V_i^w - C_{CO2} \cdot e \cdot (Q_i^{fuel}) - O\&M_{var} \quad (4)$$

The first term in (4) represents the revenues from selling on the market the net power output, i.e., the algebraic sum of CCGT, HP, and electric heater power. The second term represents the cost of fuel, then two different start-ups are considered, hot (hs) and warm (ws), C is the cost associated with the start-up and V is a binary logic variable. The cost associated with CO_2 emission is computed as the unitary cost of allowance times the emission factor *e* times the fuel consumption. Finally, Operation and Maintenance costs are included.

For the other storage technologies, a linear Programming (LP) optimizer is proposed. The problem is formulated by equation (5). x represent the array of solutions, the first 37 elements are the solution itself, i.e., the State of Charge (SOC) before and after each of the 36 time intervals, elements from 38 to 73 represent the values of the first auxiliary variable (C_{degr}) dealing with the cost associate with degradation at each time step, finally, elements from 74 to 109 represent the second auxiliary variable (C_{ineff}) dealing with the cost of charge and discharge inefficiency at each time step.

$$\min_x f^T x \ s.t. \begin{cases} A \cdot \mathrm{x} \leq \mathrm{b} \\ A_{eq} \cdot \mathrm{x} = b_{eq} \\ lb \leq \mathrm{x} \leq \mathrm{u}b \end{cases} \quad (5)$$

$$x^T = \left(SOC_1 \quad \dots \quad SOC_{37} \quad , C_{degr_1} \quad \dots \quad C_{degr_{36}} \quad , C_{ineff_1} \quad \dots \quad C_{ineff_{36}}\right) \quad (6)$$

f is the array of coefficients of objective function expressing the linear dependence between the solution array x and objective, i.e., the sum of net operational profits over the optimization period.

The first 37 elements of f directly link the SOC and revenues from discharging and the cost due to charging, while the elements from 38 to 109 are equal to -1.

$$f^T = \left(\left(-p_{el_1}\right) \cdot \frac{E_{max}}{100} \quad \left(p_{el_1} - p_{el_2}\right) \cdot \frac{E_{max}}{100} \quad \dots \quad \left(p_{el_{36}}\right) \cdot \frac{E_{max}}{100} \quad , \quad -1 \quad \dots \quad -1 \, , \quad -1 \quad \dots \quad -1\right) \quad (7)$$

The linear constraints, expressed by the matrix A and array b, relate the auxiliaries variables C_{degr} and C_{ineff} to the difference of SOC within the relative time interval. More in detail 5 different types of constraints are imposed. The two first limits the maximum difference, respectively upward (equation(8)) and downward (equation (9)), the limit is imposed by the maximum admissible power (even expressed as C-rate for BESS) during charge and discharge. These constraints are expressed by means of the time constant τ, i.e., the minimum time [h] required by a complete charge or discharge, equal to the ratio between nominal capacity E_{max} and the maximum charging and discharging power.

$$SOC_i - SOC_{i-1} \leq \frac{100}{\tau_{ch}} \quad (8)$$

$$SOC_{i-1} - SOC_i \leq \frac{100}{\tau_{disch}} \quad (9)$$

Secondly, matrix A imposes the C_{degr} at each time interval. For some kinds of storage, such as BES, lifetime is determined by the maximum number of cycles. Consequently operating the storage has a cost since once the maximum number of equivalent cycles is reached the storage must be replaced paying again the CAPEX. Each equivalent cycle has, therefore, a cost equal to the ratio between CAPEX and the maximum number of equivalent cycles, equation(10), then the degradation cost at the time interval i depends on the fraction of equivalent cycle performed on that interval, equation (11).

$$C_{cycle} = \frac{CAPEX}{N_{cycle_{max}}} \quad (10)$$

$$C_{degr_i} \geq C_{cycle} \cdot \frac{|SOC_{i+1} - SOC_i|}{100} \quad (11)$$

Finally, the cost of charging and discharging efficiency is considered.

$$C_{inef_i} \geq \begin{cases} (SOC_{i+1} - SOC_i) \cdot p_{el_i} \cdot \frac{E_{max}}{100} \cdot \left(\frac{1}{\eta_{ch}} - 1\right), & (SOC_{i+1} - SOC_i) > 0 \\ (SOC_i - SOC_{i+1}) \cdot p_{el_i} \cdot \frac{E_{max}}{100} \cdot (\eta_{disch} - 1), & (SOC_{i+1} - SOC_i) < 0 \end{cases} \quad (12)$$

Furthermore, A_{eq} and b_{eq} impose the SOC at the initial time: for the first optimization, the minimum SOC allowed is used, while for the subsequent optimizations the SOC_{25} of the previous day is set. Lower bounds and upper bounds are imposed consistently as follows.

$$lb^T = (100 - DoD_{max} \quad \dots \quad 100 - DoD_{max} \, , \quad 0 \quad \dots \quad 0, \quad 0 \ \dots \ 0) \quad (13)$$

$$ub^T = (100 \quad \dots \quad 100, \quad inf \quad \dots \quad inf, \quad inf \quad \dots \quad inf) \quad (14)$$

https://doi.org/10.52202/069564-0213

3. Storage preliminary sizing

The ICU-CCGT integration design is a fairly complex process that must take into account the site market and meteorological specificity, even when focusing on just continuous cooling [43]. However, the size indicated by previous works (i.e., 10 MWh and 10 MW of Thermal Energy Storage and a 3.5 MW Heat Pump) as the preferable value was used to maintain comparable results. The corresponding CAPEX has been estimated at 6.3 M€ [36,44]. To proceed to a fair comparison between this solution and pure storage technologies a preliminary sizing of the latter is required.

Sizing is diriment because it directly impacts capital expenditure. The overall CAPEX depends on the storage size [MWh], the charging, and the discharging power [MW]. Table 1 reports assumed values for this paper from an existing literature survey. As a consequence, the specific CAPEX [€/kWh] depends on the storage duration τ_{disch} and the ratio between charging and discharging time constant, τ_{ratio}. Figure 2 shows the trend of specific CAPEX versus τ_{disch} considering τ_{ratio} between 1 and 6. However, BES CAPEX is typically expressed as an exclusive function of the storage capacity since capacity and power are strictly correlated and typically increased power does not imply extra costs, especially considering that if an hourly time interval is assumed, as in this paper, there is no advantage in adopting C-rate beyond 1 that are therefore not investigated. Thus BES curve in Figure 2 is flat.

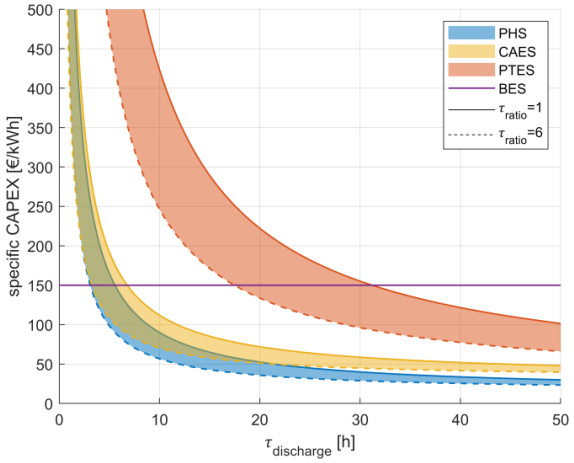

Figure. 2. Storage specific CAPEX versus duration of discharge

Figure 2 shows that BESs are the most economical storage for a short duration, generally, the other technologies CAPEX are very sensitive to the duration when it drops below 10h since the cost of power units becomes predominant. Increasing τ_{ratio} leads to savings in CAPEX decoupling charging and discharging power. Charging equipment cost weights more than the discharging one, so the impact of the τ_{ratio} is crucial in balancing the effect of reducing the CAPEX by decreasing the size of the charging equipment by a factor $1/\tau_{ratio}$, while increasing the operational charging time accordingly. This can be exploited if the duration of the off-peak price period is greater than the peak duration and if the off-peak price profile is constant, so $\tau_{ratio}>1$ is not directly reflected in an OP decrease. For a short duration, capital expenditure implied by CAES and PHS are comparable, nevertheless considering increased τ values the weight of storage cost itself is much more relevant if compared to the charging and discharging power units CAPEX, consequently in this case PHS is more advantageous because the cost per kWh is almost half of CAES.

Table 1. Technical and economic assumptions for each storage technology

	BESS	PHS	CAES	PTES
E_{max} [MWh]	1MWh	7 GWh	250 MWh	250 MWh
DoD_{max}	80%	90%	50%	100%
τ_{disc} [h]	1	2-24	2-24	2-24
$\tau_{ch\ min}$ / $\tau_{disch\ min}$	1	1-6	1-6	1-6
η_{ch}	92%	85%	75%	200%
η_{disch}	92%	88%	85%	30%
$CAPEX_{storage}$	150€/kWh	15€/kWh	32€/KWh	21€/KWh
$CAPEX_{ch}$	-	400€/kW	500€/kW	2125€/kW
$CAPEX_{disch}$	-	350€/kW	300€/kW	1900€/kW
Lifetime_max	25yr	80yr	35yr	35yr
$N_{cycle\ max}$	7500	-	-	-
ref	[28,45]	[46]	[46]	[47]

https://doi.org/10.52202/069564-0213

To preliminary size BES, PHS, CAES, and PTES, yearly optimizations are performed to quantify OP, PBP, and IRR. Different scenarios have been investigated, considering years from 2018 to 2022 and the 9 market zone identified as a relevant statistical sample for the ICU-CCGT integration [38]. The driving market factor for energy arbitrage is the price difference that can be exploited. Equation (15) expresses in a general form the minimum discharge price to be worth operating storage, it depends on the charging price, the efficiency of charging and discharging, and the degradation costs.

$$p_{el_{disch}} > \frac{C_{degr}}{\eta_{disch}} + \frac{p_{el_{ch}}}{\eta_{disch}\eta_{ch}} \tag{15}$$

Therefore to characterize each market scenario the average daily variability $\overline{\Delta p_{el_d}}$ is adopted highlighting the distance between the discharging price $p_{el_{disch}}$ and the charging price, $p_{el_{ch}}$, on a daily basis. Table 2 reports the values of $\overline{\Delta p_{el_d}}$ and the yearly average price, $\overline{p_{el_y}}$, for each year and zone. Optimizations have been performed considering data synthesized in Table 1 as input of the LP scheduler described in the Methodology section.

Table 2. Average daily electricity price spread and yearly price average [€/MWh] in the considered years and zones.

Bidding Zone	State/ Country	Ref. Location	2018		2019		2020		2021		2022	
			$\overline{\Delta p_{el_d}}$	$\overline{p_{el_y}}$	$\overline{\Delta p_{el_d}}$	$\overline{p_{el_y}}$	$\overline{\Delta p_{el_d}}$	$\overline{p_{el_y}}$	$\overline{\Delta p_{el_d}}$	$\overline{p_{el_y}}$	$\overline{\Delta p_{el_d}}$	$\overline{p_{el_y}}$
ARKANSAS_HUB	AR	Pine Bluff	21.64	25.03	15.67	21.27	13.83	17.72	24.29	31.05	44.87	56.81
AT	AT	Vienna	31.15	46.32	26.72	40.06	28.25	33.14	72.32	106.85	163.51	261.4
CENTRL	NY	Syracuse	48.87	50.38	33.52	40.00	14.74	17.40	49.60	57.42	107.56	123.35
LZ_CPS	TX	San Antonio	73.52	29.41	137.54	35.70	40.28	20.15	113.63	123.85	125.88	63.65
NEWHAMPSHIRE	NH	Manchester	29.92	37.32	20.95	28.13	19.29	22.01	29.57	39.09	59.98	81.56
NO3	NO	Trondheim	13.10	44.08	8.81	38.54	3.61	9.46	21.58	41.07	40.04	41.94
NORD	IT	Milan	31.28	60.71	28.05	51.25	26.06	37.79	59.40	125.2	161.52	307.81
SCE	CA	Los Angeles	60.13	37.28	49.52	33.13	69.16	31.13	65.64	43.60	99.56	82.07
SICI	IT	Palermo	56.99	69.49	71.75	62.77	48.87	46.21	73.15	129.02	172.8	295.07

Table 3 reports the Utilization Factor (UF) as the first output of storage dispatch optimizations, the reported τ_{disch} and τ_{ratio} are selected as the best in the following economic analysis for each storage technology. The UF is defined as the ratio between the discharged energy and the energy discharged if a cycle until the maximum allowed depth of discharge was performed daily.

$$UF = \frac{\sum_1^{n_{days}} E_{disch}}{E_{max} \cdot \frac{DoD_{max}}{100} \cdot n_{days}} \tag{16}$$

Table 3. UF [-] computed on a yearly basis for the best storage duration

Bidding Zone (State/Country)	BES τ_{disch}=1h τ_{ratio} =1					PHS τ_{disch}=12h τ_{ratio} =1					CAES τ_{disch}=12h τ_{ratio} =1					PTES τ_{disch}=2h τ_{ratio} =1				
	2018	2019	2020	2021	2022	2018	2019	2020	2021	2022	2018	2019	2020	2021	2022	2018	2019	2020	2021	2022
ARKANSAS_HUB (AR)	0.339	0.156	0.101	0.372	0.760	0.765	0.701	0.743	0.734	0.745	1.006	0.952	0.982	0.977	0.969	0.001	0	0.002	0.002	0
AT (AT)	0.55	0.449	0.461	1.127	1.686	0.730	0.716	0.749	0.734	0.717	1.091	1.070	1.134	1.107	1.055	0.101	0.096	0.126	0.076	0.042
CENTRL (NY)	0.871	0.656	0.105	0.862	1.275	0.788	0.743	0.554	0.755	0.749	1.066	1.012	0.781	1.025	1.019	0.016	0.001	0.004	0.001	0.003
LZ_CPS (TX)	0.741	0.722	0.536	0.805	1.145	0.820	0.817	0.815	0.828	0.85	1.057	1.064	1.035	1.084	1.131	0.042	0.094	0.021	0.044	0.079
NEWHAMPSHIRE (NH)	0.507	0.282	0.270	0.552	1.171	0.750	0.737	0.761	0.730	0.720	1.037	1.062	1.078	1.059	1.042	0.008	0.004	0.004	0.004	0.004
NO3 (NO)	0.125	0.038	0.008	0.253	0.387	0.355	0.301	0.455	0.476	0.546	0.450	0.356	0.566	0.605	0.696	0.020	0.011	0.01	0.03	0.066
NORD (IT)	0.599	0.545	0.493	0.912	1.557	0.575	0.666	0.692	0.597	0.611	0.846	0.973	1.034	0.879	0.902	0.001	0.007	0.021	0.007	0.008
SCE (CA)	1.064	1.088	0.962	1.037	1.207	0.866	0.867	0.865	0.855	0.842	1.239	1.256	1.231	1.210	1.159	0.097	0.151	0.211	0.159	0.164
SICI (IT)	1.266	1.401	1.122	1.239	1.636	0.788	0.827	0.828	0.686	0.639	1.196	1.263	1.268	1.028	0.959	0.031	0.111	0.057	0.043	0.074

Table 3 indicates that the highest UFs are reported by BES in 2022, under considerably favorable market conditions. This occurs especially in those bidding zones, typically as southern and central Europe, characterized by two distinct and prominent price peaks, in the morning and early evening, and presenting the opportunity to perform two cycles in a day. On the opposite side, other markets, e.g. Texas, even characterized by a relevant daily variability, typically show only one peak in a day, thus the second daily

https://doi.org/10.52202/069564-0213

discharge is very rare. Finally, markets characterized by flat electricity price and reduced variability, e.g., Norway, shows reduced potential for arbitrage for all the storage technologies.

If BES scored the UF highest values, CAES UF is considerably robust (around 1) even under less favorable market scenarios. However, CAES is characterized by a very low allowed DoD (50%), which means that, designing τ_{disch}=12h, just 6h are required to discharge until the maximum allowed depth. 12h and 10.8h are required by PTES and PHS respectively. The operativity of storage would depend only on the frequency with equation (15) is satisfied, consequently BES has a great advantage thanks to high efficiency, and low τ_{disch} and τ_{ch} but, differently than other technologies, it pays the impact of degradation costs, especially in low and moderately variable markets. If the amount of energy discharged is considered, PHS operates more than CAES because of the highest efficiency, while PTES is almost unutilized because of the too low efficiency and therefore excluded by the following analyses.

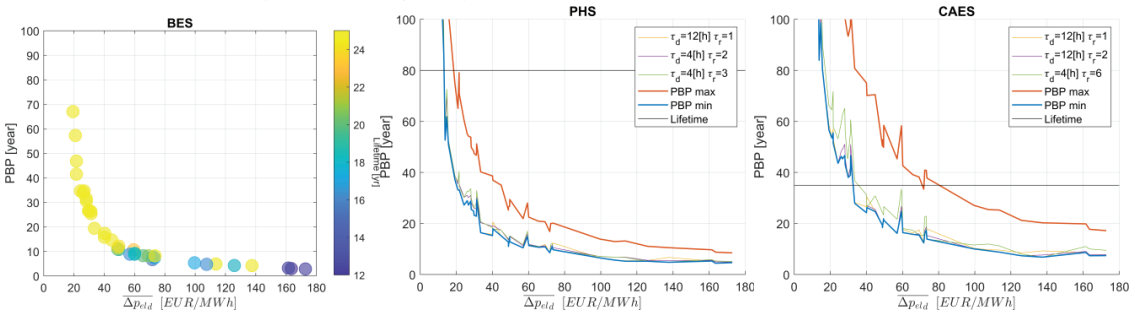

Figure. 3. BES, PHS, and CAES Pay Back Period (PBP) vs the average daily variability of electricity price

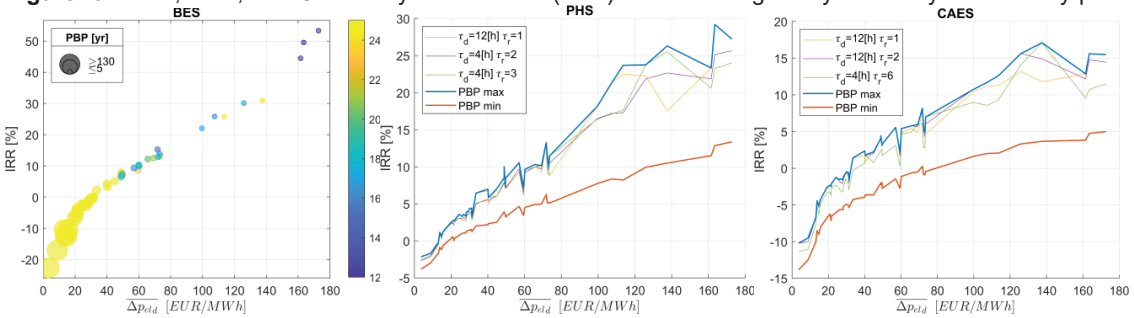

Figure. 4. BES, PHS, and CAES Internal Rate of Return (IRR) vs the average daily variability of electricity price

Figures 3 and 4 show the PBP and the IRR assessed by means of the annual cash flow, as an output of the yearly optimizations. Consequently, trends are drawn considering 45 values and the relative $\overline{\Delta p_{el_d}}$, from 5 years and 9 bidding zone reported in Table 2. Trends appear smooth enough to confirm the outcome of [38], identifying $\overline{\Delta p_{el_d}}$ as the best predictor for energy storage economic performance.

BESs present the lowest PBP; for $\overline{\Delta p_{el_d}}$ >50-55 €/MWh it drops below 10 years, however, the expected lifetime reduces as well because of the increased utilization. Besides the cycling aging of BES, calendar aging must be considered. According to the model presented by Stroe et al. [28], the maximum calendar life for an idling battery is about 25 years, this value is assumed as ceil even if the maximum number of cycles is not reached. Such an underutilization is typical of those markets with daily variability below 50€/MWh. The IRR increases with $\overline{\Delta p_{el_d}}$ and it is positive beyond 30€/MWh of daily variability.

For PHS and CAES the ranges of τ_{disc} and τ_{ratio} (i.e., the ratio between τ_{ch} and τ_{disc}) indicated in Table 1 are investigated. The blue and the red lines in Figures 3 and 4 represent the envelope of best and worst points respectively, moreover, three other lines are plotted for the three combinations of τ_{disc} and τ_{ratio} that more often result as the best possible. Both for PHS and CAES the best couple is τ_{disc}=12h and τ_{ratio}=1, while the second and the third rank differ for the two technologies showing that selecting τ_{ch} about 12-24h is preferable for CAES to limit CAPEX. PBP shows similar trends for CAES and PHS, even if under extremely favorable conditions (right side of charts) the PBP stabilizes at a slightly lower value for PHS (about 5 years, while 8 years are required to pay back the CAES) because of the lower specific CAPEX, as shown by Figure 1, and the higher efficiency. Moreover, it must be considered that the expected lifespan is significantly higher for PHS and this is reflected in the IRR which is positive even for reduced $\overline{\Delta p_{el_d}}$ (>10-15€/MWh).

For the purpose of the comparison between traditional storage technologies and the CCGT-ICU integration in Section 3, the best τ_{disc} and τ_{ratio} are selected.

4. ICU-CCGT comparison

The comparison is carried out on the three market zones that showed the highest potential for the integration of an ICU in an existing CCGT: SCE in California, northern Italy (NORD), and LZ_CPS in Texas[i] [38]. Respective reference locations for historical climate data are Los Angeles, Milan, and San Antonio. The previous section highlights how the bidding zone is not relevant for BES, PHS, and CAES but what is diriment is the exploitable variability in electricity price on a daily basis. Thus, for these technologies, is proposed an aggregated analysis, Figure 5 shows trend lines both for PBP and IRR built on rational 3rd-degree function fitting all 45 available values.

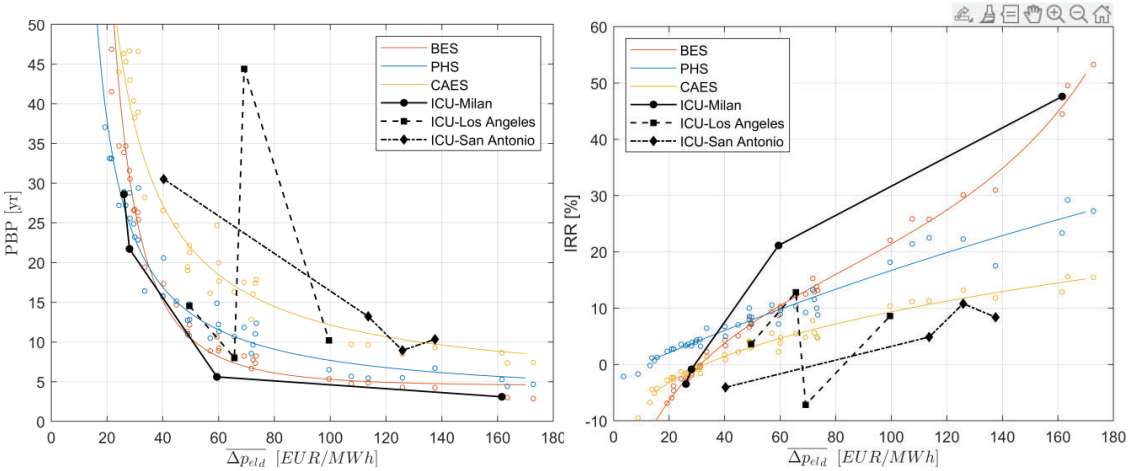

Figure. 5. PBP and IRR comparison for BES, PHS, CAES, and ICU-CCGT in three different locations

The analysis reported in a previous paper [38], was focused on one year and highlighted structural differences between market zone clusters considering both markets and climate parameters. On the other hand, this paper considers several years of operations highlighting that for systems with ICUs, an in-depth analysis is necessary and the expected economic outcome it is difficult to generalize because of the additional influence of ambient temperature and, secondly, of electricity price-gas price relationship, often synthesized by the Clean Spark Spread, the difference between the electricity price and the CCGT production cost, including CO_2, as defined in eq. (18). However, $\overline{\Delta p_{el_d}}$ confirms to be an effective indicator and the economic performance constantly improves as it increases. The only exception is represented by Los Angeles in 2020 due to the low Clean Spark Spread that year.

Even if in Texas and California higher $\overline{\Delta p_{el_d}}$ values are more common historically, for the same value the ICU-CCGT potential is higher in northern Italy. As Confirmed by Figure 6 and Table 4, in this location the potential for using directly the HP for heating and cooling the inlet air is higher (about 30% of operating hours for each of these operational modes), conversely, the TES is more exploited in California and Texas. In this last location is common to discharge the TES more than once a day and the inlet cooling by means of TES discharging is adopted for about 15% of operational modes. Despite the typical single peak price profile of this zone, this is possible because the value of energy discharged by the TES depends both on the electricity price and the potential CCGT power increase following the cooling depending on the ambient temperature. Thus, if the daily trends of ambient temperature and electricity price present two peaks characterized by sufficient prominence and temporal shifting, the resulting profits opportunities may result in a two peaks profile allowing a UF beyond 1.

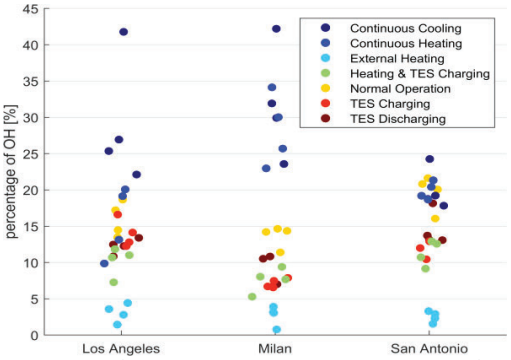

Table 4. Inlet Conditioning Unit TES UF [-]

	Bidding Zone (State/Country)		
	SCE (CA)	NORD (IT)	LZ_CPS (TX)
2019	0.706	0.372	1.01
2020	0.627	0.311	1.032
2021	1.056	0.783	1.548
2022	0.819	0.5991	1.139

Figure. 6. Operating mode as a percentage of overall operating hours

https://doi.org/10.52202/069564-0213

More in detail, from an economic perspective the main difference between the ICU-CCGT integration and the other storage technologies relies on the value at which the discharging power is awarded. The thermal energy discharged by the TES is reflected in an extra power output of the CCGT and a slight variation in efficiency since the fuel consumption increases as well, a detailed investigation of the dependence on the ambient temperature and the GT load is provided in [35]. Thus the economic value of the discharged energy is the power increment, due to inlet cooling by TES discharging, times the Clean Spark Spread (CSS), i.e., the profit margin of a CCGT power plant considering the fuel consumption and the cost of carbon dioxide allowance emissions, equation (18). Conversely, the cost of charging the TES is proportional to the ratio of electricity price on the HP COP. Analogously to equation (15), is possible to state the minimum condition to be worth operating the TES of an ICU. For the sake of simplicity, equation (17) neglects the variation in efficiency and thus in CSS following the TES discharge.

$$\Delta P \cdot CSS_{disch} = E_{disch} \cdot f(T_{amb}, Load_{GT}) \cdot CSS_{disch} \geq \frac{E_{disch} \cdot p_{el_{ch}}}{COP(T_{amb})} \tag{17}$$

$$CSS = p_{el} - C_{gas} \cdot \left(\frac{1}{\eta_{CCGT}} - C_{CO2} \cdot e \right) \tag{18}$$

Finally, Figure 7 confirms the pivotal importance of CSS reporting the boxplot distributions versus $\overline{\Delta p_{el_d}}$ for each year in the analyzed locations, in the hours in which the TES is discharged, CSS_{disch}. It is immediate to appreciate the strict correlation between the trend lines connected the CSS median values and the IRR or the opposite of PBP in Figure 5. CSS can be considered as a carrier signal, then on the right part of the chart trends diverge because the extra benefits on economic KPIs of increased $\overline{\Delta p_{el_d}}$.

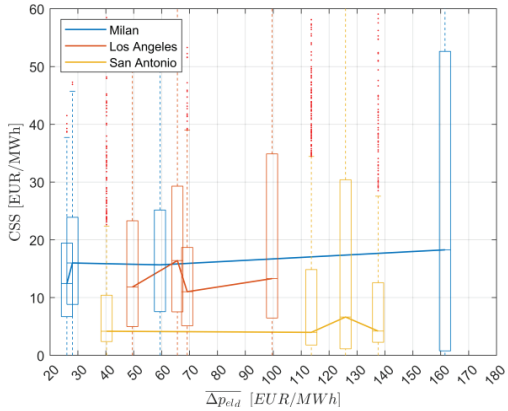

Figure. 7. Yearly Clean Spark Spread distribution versus the average daily variability

5. Conclusions

This paper performs a market analysis by means of Linear Programming and Mixed Integer Linear Programming optimizer of different storage technologies for energy arbitrage on the day-ahead market. Battery Energy Storage (BES), Pumped Hydro Storage (PHS), Compressed Air Energy Storage (CAES), and Pumped Thermal Energy Storage (PTES) are compared against the integration of a Combined Cycle Gas Turbine with an Inlet Conditioning Unit consisting of a Heat Pump and a cold Thermal Energy Storage (CCGT-ICU). Different scenarios have been analyzed considering historical data from different bidding zones and years.

First, it was observed how the operativity of energy storage depends on the conversion efficiency and any possible cost associated with the degradation of the storage itself, this is an important issue for batteries. It was observed that PTES presents a very low utilization factor, because of the low round trip efficiency profit opportunities from arbitrage with PTES are very rare and it is not possible to pay the investment back. PTES is then excluded by the following analysis.

A sizing procedure applied to PHS and CAES identifies both an optimal charging and discharging duration of about 12h, highlighting how limiting the charging power is an effective approach to reduce CAPEX and enhance economic KPIs. The daily electricity price variability is the driving factor for storage opportunities. Thanks to the absence of degradation costs and a good round trip efficiency, PHS performs better on markets characterized by moderate variability (<40-60 €/MWh), while batteries are the best solutions when the price is extremely variable (>60 €/MWh), in such a condition the high efficiency represents an advantage despite the cost associated to the storage degradations; performing even two cycles per day. CAES may find an application in low variable markets (<30-40 €/MWh), if there is no site availability for PHS. However in such conditions, the PBP is close to the expected lifespan, thus the viability of investment for CAES is still uncertain if only arbitrage profits are considered.

Introducing the ICU-CCGT integration in the comparison requires separately analyzing bidding zones because of the impact of local climate and the Clean Spark Spread (CSS). The proposed integration wins

the comparison against other storage technologies in northern Italy and demonstrates to be competitive in California while it shows lower performance in Texas. It was demonstrated that what drastically impacts this outcome is the CSS and the opportunities to use the ICU also for direct inlet cooling and heating.

It is possible to conclude that, as pure storage, the ICU integration presents low performance if compared to a system designed for this purpose. However, within the ICU investment, an HP is included that, if exploited in continuous heating and cooling mode, can increase the extra profits generated by the ICU retrofitting. Moreover, it must be considered that such an investment can avoid the closure or mothballing of the CCGT power plant, therefore keeping available to the Transmission System Operator a relevant capacity for supplying services to the grid, including the rotational inertia typical of turbomachinery-based power plants and essential for the purpose of frequency regulation.

Nomenclature

Acronyms

BES	Battery Energy Storage
CAPEX	Capital Expenditure
CAES	Compressed Air Energy Storage
CCGT	Combined Cycle Gas Turbine
GT	Gas Turbine
HP	Heat Pump
HX	Heat Exchanger
ICU	Inlet Conditioning Unit
LP	Linear Programming
MILP	Mixed Integer Linear Programming
OH	Operating Hours
PHS	Pumped Hydro Storage
PTES	Pumped Thermal Energy Storage
RES	Renewable Energy Sources
TES	Thermal Energy Storage

Variables

C	Cost, €, €/MWh, €/ton
COP	Coefficient of Performance, -
CSS	Clean Spark Spread, €/MWh
DoD	Depth of Discharge, %
e	Emission factor, ton/MWh
E	energy, MWh
i	Interest rate, -
IRR	Internal Rate of Return, %
O&M	Operating and Maintenance Costs, €/MWh
OP	Operational Profits, €
P	Power, MW
p	Price, €/MWh
PBP	Pay Back Period, yr
Q	Quantity, MWh
RTE	Round Trip Efficiency, %
SOC	State of Charge, %
T	Temperature, °C
UF	Utilization Factor, -
V	Start-up Binary Variable, logic
η	Efficiency, %
τ	Duration, h

Subscripts and superscripts

amb	Ambient
d	Daily
el	Electricity
ch	Charge
disch	Discharge
T	Transpose
inef	Inefficiency
degr	Degradation
w	Warm
h	Hot
s	Start-up

https://doi.org/10.52202/069564-0213

References

[1] Tavoni M, Kriegler E, Riahi K, Van Vuuren DP, Aboumahboub T, Bowen A, et al. Post-2020 climate agreements in the major economies assessed in the light of global models. Nat Clim Chang 2015;5:119–26. https://doi.org/10.1038/nclimate2475.

[2] Lang J, Hyslop C, Yeo XY, Black R, Chalkley P, Hale T, et al. Net Zero Tracker 2023.

[3] International Energy Agency. World Energy Outlook 2022. Paris: 2022.

[4] Yasmina Abdelilah, Heymi Bahar, Trevor Criswell, Piotr Bojek, François Briens. Renewables 2022: analysis and forecast to 2027. Paris: 2022.

[5] Ramsebner J, Haas R, Ajanovic A, Wietschel M. The sector coupling concept: A critical review. WIREs Energy Environ 2021;10:e396. https://doi.org/https://doi.org/10.1002/wene.396.

[6] Aslam S, Herodotou H, Mohsin SM, Javaid N, Ashraf N, Aslam S. A survey on deep learning methods for power load and renewable energy forecasting in smart microgrids. Renew Sustain Energy Rev 2021;144:110992. https://doi.org/https://doi.org/10.1016/j.rser.2021.110992.

[7] Corizzo R, Ceci M, Fanaee-T H, Gama J. Multi-aspect renewable energy forecasting. Inf Sci (Ny) 2021;546:701–22. https://doi.org/https://doi.org/10.1016/j.ins.2020.08.003.

[8] Ramesh AV, Li X. Reducing Congestion-Induced Renewable Curtailment with Corrective Network Reconfiguration in Day-Ahead Scheduling. 2020 IEEE Power Energy Soc. Gen. Meet., 2020, p. 1–5. https://doi.org/10.1109/PESGM41954.2020.9281399.

[9] Yasuda Y, Bird L, Carlini EM, Eriksen PB, Estanqueiro A, Flynn D, et al. C-E (curtailment – Energy share) map: An objective and quantitative measure to evaluate wind and solar curtailment. Renew Sustain Energy Rev 2022;160:112212. https://doi.org/https://doi.org/10.1016/j.rser.2022.112212.

[10] Bouakkaz A, Mena AJG, Haddad S, Ferrari ML. Efficient energy scheduling considering cost reduction and energy saving in hybrid energy system with energy storage. J Energy Storage 2021;33:101887. https://doi.org/https://doi.org/10.1016/j.est.2020.101887.

[11] Rehman S, Al-Hadhrami LM, Alam MM. Pumped hydro energy storage system: A technological review. Renew Sustain Energy Rev 2015;44:586–98. https://doi.org/https://doi.org/10.1016/j.rser.2014.12.040.

[12] Deane JP, Ó Gallachóir BP, McKeogh EJ. Techno-economic review of existing and new pumped hydro energy storage plant. Renew Sustain Energy Rev 2010;14:1293–302. https://doi.org/https://doi.org/10.1016/j.rser.2009.11.015.

[13] Guittet M, Capezzali M, Gaudard L, Romerio F, Vuille F, Avellan F. Study of the drivers and asset management of pumped-storage power plants historical and geographical perspective. Energy 2016;111:560–79. https://doi.org/https://doi.org/10.1016/j.energy.2016.04.052.

[14] Kougias I, Szabó S. Pumped hydroelectric storage utilization assessment: Forerunner of renewable energy integration or Trojan horse? Energy 2017;140:318–29. https://doi.org/https://doi.org/10.1016/j.energy.2017.08.106.

[15] Schill W-P, Kemfert C. Modeling Strategic Electricity Storage: The Case of Pumped Hydro Storage in Germany. Energy J (Cambridge, Mass) 2011;32:59–87. https://doi.org/10.5547/ISSN0195-6574-EJ-Vol32-No3-3.

[16] Connolly D, MacLaughlin S, Leahy M. Development of a computer program to locate potential sites for pumped hydroelectric energy storage. Energy 2010; 35:375–81. https://doi.org/https://doi.org/10.1016/j.energy.2009.10.004.

[17] McLean E, Kearney D. An Evaluation of Seawater Pumped Hydro Storage for Regulating the Export of Renewable Energy to the National Grid. Energy Procedia 2014;46:152–60. https://doi.org/https://doi.org/10.1016/j.egypro.2014.01.168.

[18] International Energy Agency. Grid-Scale Storage. Paris: 2022.

[19] U.S. Department of Energy. Battery Storage in the United States: An Update on Market Trends. 2021.

[20] Farhadi M, Mohammed O. Energy Storage Technologies for High-Power Applications. IEEE Trans Ind Appl 2016;52:1953–62. https://doi.org/10.1109/TIA.2015.2511096.

[21] Argyrou MC, Christodoulides P, Kalogirou SA. Energy storage for electricity generation and related processes: Technologies appraisal and grid scale applications. Renew Sustain Energy Rev 2018;94:804–21. https://doi.org/https://doi.org/10.1016/j.rser.2018.06.044.

[22] Rancilio G, Lucas A, Kotsakis E, Fulli G, Merlo M, Delfanti M, et al. Modeling a Large-Scale Battery Energy Storage System for Power Grid Application Analysis. Energies 2019;12. https://doi.org/10.3390/en12173312.

[23] Dunn B, Kamath H, Tarascon J-M. Electrical Energy Storage for the Grid: A Battery of Choices. Science (80-) 2011;334:928–35. https://doi.org/10.1126/science.1212741.

[24] Gallo AB, Simões-Moreira JR, Costa HKM, Santos MM, Moutinho dos Santos E. Energy storage in the energy transition context: A technology review. Renew Sustain Energy Rev 2016;65:800–22. https://doi.org/https://doi.org/10.1016/j.rser.2016.07.028.

[25] May GJ, Davidson A, Monahov B. Lead batteries for utility energy storage: A review. J Energy Storage 2018;15:145–57. https://doi.org/https://doi.org/10.1016/j.est.2017.11.008.

[26] Sánchez-Díez E, Ventosa E, Guarnieri M, Trovò A, Flox C, Marcilla R, et al. Redox flow batteries: Status and perspective towards sustainable stationary energy storage. J Power Sources 2021;481:228804. https://doi.org/https://doi.org/10.1016/j.jpowsour.2020.228804.

[27] Fan X, Liu B, Liu J, Ding J, Han X, Deng Y, et al. Battery Technologies for Grid-Level Large-Scale Electrical Energy Storage. Trans Tianjin Univ 2020;26:92–103. https://doi.org/10.1007/s12209-019-00231-w.

[28] Stroe DI, Knap V, Swierczynski M, Stroe AI, Teodorescu R. Operation of a grid-connected lithium-ion battery energy storage system for primary frequency regulation: A battery lifetime perspective. IEEE Trans Ind Appl 2017;53:430–8. https://doi.org/10.1109/TIA.2016.2616319.

[29] Houssainy S, Janbozorgi M, Kavehpour P. Thermodynamic performance and cost optimization of a novel hybrid thermal-compressed air energy storage system design. J Energy Storage 2018;18:206–17. https://doi.org/https://doi.org/10.1016/j.est.2018.05.004.

[30] Bazdar E, Sameti M, Nasiri F, Haghighat F. Compressed air energy storage in integrated energy systems: A review. Renew Sustain Energy Rev 2022;167:112701. https://doi.org/10.1016/j.rser.2022.112701.

[31] Aghahosseini A, Breyer C. Assessment of geological resource potential for compressed air energy storage in global electricity supply. Energy Convers Manag 2018;v. 169:161-173–2018 v.169. https://doi.org/10.1016/j.enconman.2018.05.058.

[32] Vecchi A, Knobloch K, Liang T, Kildahl H, Sciacovelli A, Engelbrecht K, et al. Carnot Battery development: A review on system performance, applications and commercial state-of-the-art. J Energy Storage 2022;55:105782. https://doi.org/https://doi.org/10.1016/j.est.2022.105782.

[33] Dumont O, Frate GF, Pillai A, Lecompte S, De paepe M, Lemort V. Carnot battery technology: A state-of-the-art review. J Energy Storage 2020;32:101756. https://doi.org/https://doi.org/10.1016/j.est.2020.101756.

[34] Novotny V, Basta V, Smola P, Spale J. Review of Carnot Battery Technology Commercial Development. Energies 2022;15. https://doi.org/10.3390/en15020647.

[35] Sorce A, Giugno A, Marino D, Piola S, Guedez R. Analysis of a Combined Cycle Exploiting Inlet Conditioning Technologies for Power Modulation. Proc. ASME Turbo Expo 2019 Turbomach. Tech. Conf. Expo. June 17-21 2019, Phoenix, Arizona, USA: 2019. https://doi.org/https://doi.org/10.1115/GT2019-91541.

[36] Mantilla W, Garcia J, Guédez R, Source A. Short-Term Optimization of a Combined Cycle Power Plant Integrated With an Inlet Conditioning Unit. J Eng Gas Turbines Power 2021;143. https://doi.org/10.1115/1.4050856.

[37] Vannoni A, García J, Guedez R, Sorce A. Ancillary Services Potential for Flexible Combined Cycles. ASME Turbo Expo 2021 Turbomach. Tech. Conf. Expo. June 7-11 2021, Virtual: 2021.

[38] Vannoni A, Garcia JA, Guedez R, Sorce A, Massardo AF. Combined Cycle, Heat Pump, and Thermal Storage Integration: Techno-Economic Sensitivity to Market and Climatic Conditions Based on a European and United States Assessment. ASME Pap. GT2022-82698, ASME Turbo Expo 2022, Rotterdam, The Netherlands.: 2022.

[39] LCG Consulting. Energy Online Data n.d. http://www.energyonline.com/Data (accessed March 13, 2023).

[40] ENTSO-E. ENTSO-E Transparency Platform n.d. https://transparency.entsoe.eu/transmission-domain/r2/dayAheadPrices/show (accessed March 13, 2023).

[41] Vasylyev A, Vannoni A, Sorce A. Best Practices For Electricity Generators And Energy Storage Optimal Dispatch Problems. ASME Turbo Expo 2023 Turbomach. Tech. Conf. Expo. Vol. 4 Control. Diagnostics, Instrumentation; Cycle Innov. Cycle Innov. Energy Storage; Educ. Electr. Power. June 26–30, 2023., Boston: 2023.

[42] The World Bank. State and Trends of Carbon Pricing 2017-2021. Washington DC: n.d.

[43] Giugno A, Sorce A, Cuneo A, Barberis S. Effects of market and climatic conditions over a gas turbine combined cycle integrated with a Heat Pump for inlet cooling. Appl Energy 2021;290:116724. https://doi.org/https://doi.org/10.1016/j.apenergy.2021.116724.

[44] Vannoni A, Sorce A, Traverso A, Massardo AF. Techno-Economic Analysis of Power-to-Heat Systems. E3S Web Conf 2021;03003. https://doi.org/https://doi.org/10.1051/e3sconf/202123803003.

[45] Mauler L, Duffner F, Zeier WG, Leker J. Battery cost forecasting: a review of methods and results with an outlook to 2050. Energy Environ Sci 2021;14:4712–39. https://doi.org/10.1039/D1EE01530C.

[46] Jülch V. Comparison of electricity storage options using levelized cost of storage (LCOS) method. Appl Energy 2016;183:1594–606. https://doi.org/https://doi.org/10.1016/j.apenergy.2016.08.165.

[47] Tassenoy R, Couvreur K, Beyne W, De Paepe M, Lecompte S. Techno-economic assessment of Carnot batteries for load-shifting of solar PV production of an office building. Renew Energy 2022;199:1133–44. https://doi.org/https://doi.org/10.1016/j.renene.2022.09.039.

[i] Days from February 13 and 19, 2021 have been excluded from the Texan analysis because of the exceptional energy crisis occurred during those days. Extremely high electricity prices occurred in that period cannot be considered as regular neither fully exploitable because of the generalized unavailability of many generators following the severe weather conditions.

https://doi.org/10.52202/069564-0213